Article

Cell Reports

Cellular and Molecular Responses Unique to Major Injury Are Dispensable for Planarian Regeneration

Graphical Abstract

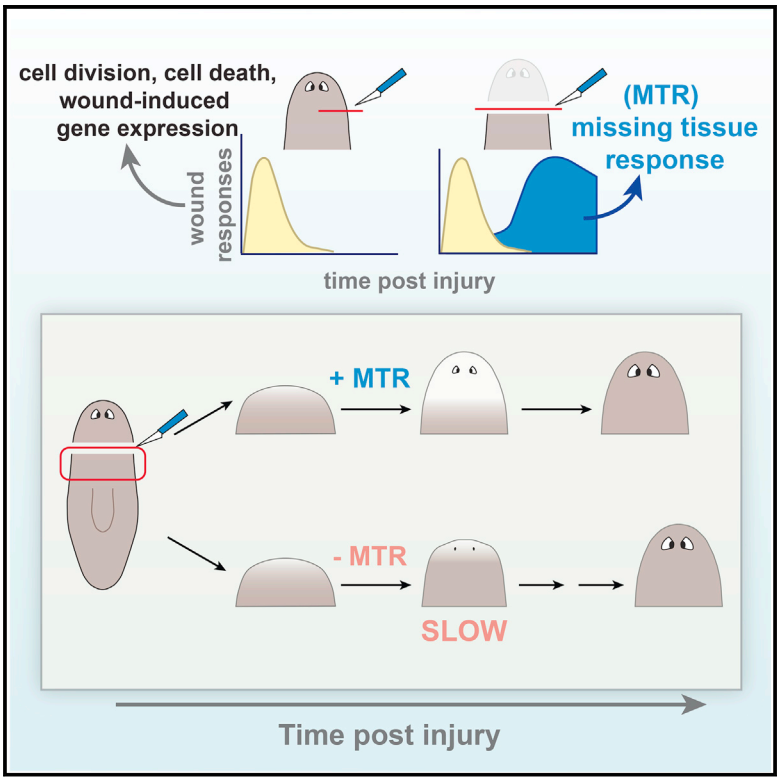

Authors

Aneesha G. Tewari, Sarah R. Stern, Isaac M. Oderberg, Peter W. Reddien

Correspondence

reddien@wi.mit.edu

In Brief

In regenerative organisms, a large array of cellular responses are triggered at major injuries. However, which of these responses are fundamentally required for regeneration to occur remains unknown. Tewari et al. find that hallmark cellular and molecular responses induced uniquely at large injuries are dispensable for planarian regeneration.

Highlights

- *follistatin* is required for the missing tissue response at many injuries
- The missing tissue response is not required for regeneration
- Regeneration occurs slowly in the absence of a missing tissue response
- *follistatin* inhibits *wnt1* at wounds to mediate its role in head regeneration

Tewari et al., 2018, Cell Reports *25*, 2577–2590
November 27, 2018
https://doi.org/10.1016/j.celrep.2018.11.004

CellPress

Cell Reports
Article

Cellular and Molecular Responses Unique to Major Injury Are Dispensable for Planarian Regeneration

Aneesha G. Tewari,[1,2] Sarah R. Stern,[1,2] Isaac M. Oderberg,[1,2,4] and Peter W. Reddien[1,2,3,5,*]
[1]Whitehead Institute for Biomedical Research, Cambridge, MA 02142, USA
[2]Department of Biology, Massachusetts Institute of Technology, Cambridge, MA 02139, USA
[3]Howard Hughes Medical Institute, Chevy Chase, MD 20815, USA
[4]Brigham and Women's Hospital, Harvard Medical School, Boston, MA 02115, USA
[5]Lead Contact
*Correspondence: reddien@wi.mit.edu
https://doi.org/10.1016/j.celrep.2018.11.004

SUMMARY

The fundamental requirements for regeneration are poorly understood. Planarians can robustly regenerate all tissues after injury, involving stem cells, positional information, and a set of cellular and molecular responses collectively called the "missing tissue" or "regenerative" response. *follistatin*, which encodes an extracellular Activin inhibitor, is required for the missing tissue response after head amputation and for subsequent regeneration. We found that *follistatin* is required for the missing tissue response regardless of the wound context, but causes regeneration failure only after head amputation. This head regeneration failure involves *follistatin*-mediated regulation of Wnt signaling at wounds and is not a consequence of a diminished missing tissue response. All tested contexts of regeneration, including head regeneration, could occur with a defective missing tissue response, but at a slower pace. Our findings suggest that major cellular and molecular programs induced specifically by large injuries function to accelerate regeneration but are dispensable for regeneration itself.

INTRODUCTION

Regeneration requires the ability to respond to injury and to replace missing body parts. How animals, such as planarians, are able to regenerate after large injuries that remove multiple tissue types is a question that has fascinated biologists for centuries. Some injuries, such as incisions, wound the animal but do not remove substantial tissue. Other injuries, such as amputations, remove significant tissue that must be replaced to return the animal to normal anatomical proportions.

Planarian regeneration requires a population of dividing stem cells called neoblasts and positional information (Reddien, 2018). Position control genes (PCGs) are regionally expressed, primarily in muscle, and are proposed to guide patterning along the body axes (Witchley et al., 2013). Substantial work has shown that a major component of regeneration after significant tissue loss is the "missing tissue," or "regenerative," response (Pellettieri et al., 2010; Wenemoser and Reddien, 2010; Wenemoser et al., 2012; Wurtzel et al., 2015; Owlarn et al., 2017).

When challenged with an injury, planarians launch a generic wound response. This response occurs rapidly, between 1 and 6 hr post wounding, and includes induction of an estimated 200+ genes, increased cell division broadly, and increased cell death near the wound (Baguñà, 1976; Saló and Baguñà, 1984; Pellettieri et al., 2010; Wenemoser and Reddien, 2010; Wenemoser et al., 2012; Wurtzel et al., 2015). These responses occur regardless of whether or not the injury is associated with substantial missing tissue. Injuries associated with substantial tissue loss induce a second set of responses collectively called the missing tissue response. Hallmarks of the missing tissue response include a second and sustained peak in mitoses near the wound, sustained expression of wound-induced genes until ~24 hr post injury, and a body-wide increase in apoptosis (Pellettieri et al., 2010; Wenemoser and Reddien, 2010; Wenemoser et al., 2012).

The gene *follistatin*, which encodes a secreted inhibitor of Activin signaling proteins, is required for the missing tissue response at anterior-facing wounds, but has no effect on the generic wound response (Gaviño et al., 2013). In addition, *follistatin* is required for anterior regeneration, with tail fragments unable to form any head structures after amputation (Gaviño et al., 2013; Roberts-Galbraith and Newmark, 2013). These observations suggested that the missing tissue response might be required for regeneration.

Although it is plausible that prominent cellular and molecular responses induced specifically by large injuries are required for regeneration, there are some indications that the missing tissue response is not required in all instances of regeneration. Planarians constantly replace adult tissues during homeostatic tissue turnover, even in the absence of injury. Specific removal of the planarian eye by surgical resection does not induce a missing tissue response, and yet eye regeneration occurs as an emergent property of constant progenitor production (LoCascio et al., 2017). In addition, although head regeneration is consistently affected by *follistatin* inhibition, tail regeneration does occur to

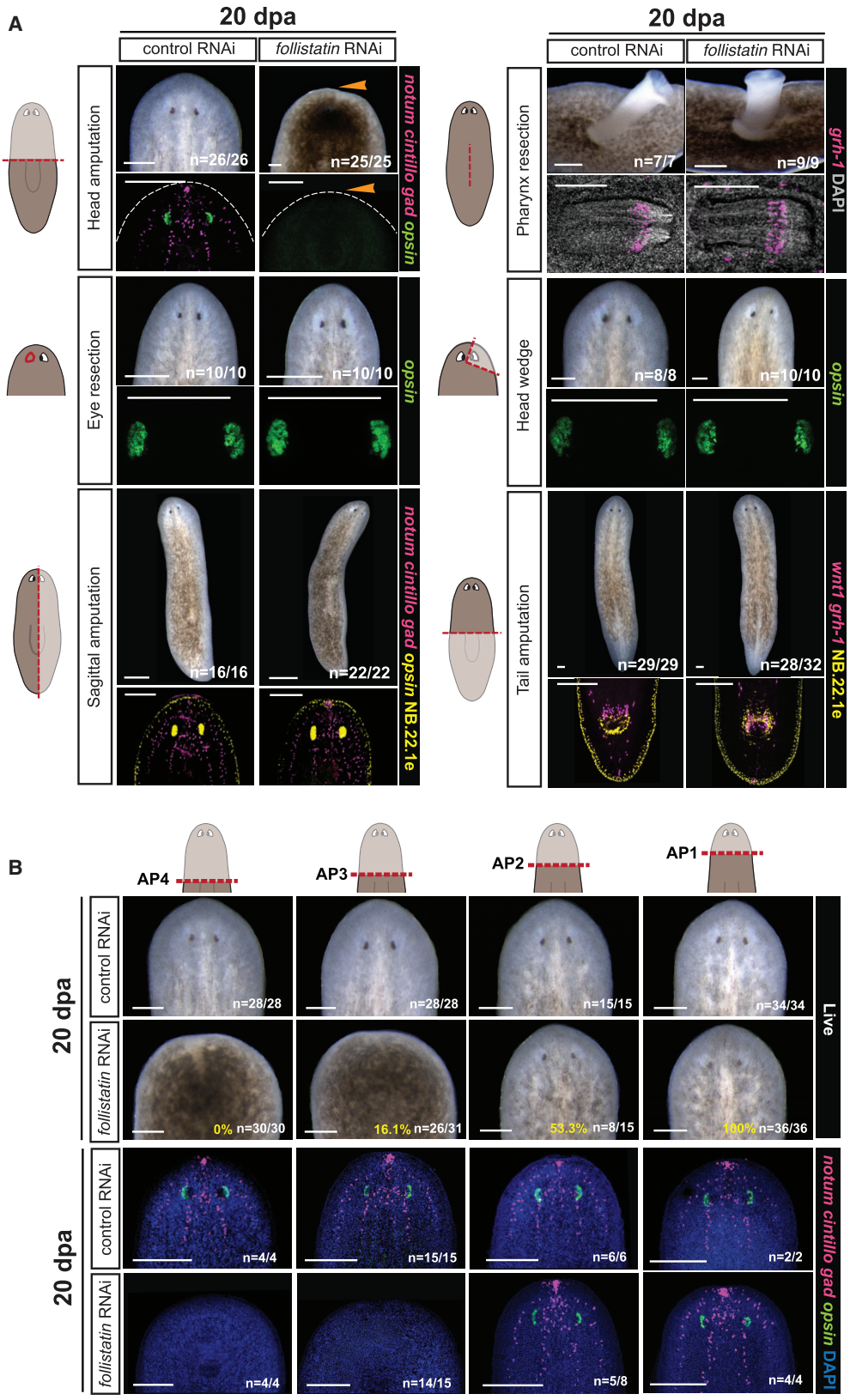

(legend on next page)

some extent by day 6 post amputation (Roberts-Galbraith and Newmark, 2013). Here we utilized inhibition of *follistatin* as a tool to disrupt induction of the missing tissue response after a wide variety of injuries. This allowed us to study the fundamental requirements of regeneration after significant tissue loss in multiple wound contexts. Our data indicate that wound-induced re-establishment of positional information can lead to regeneration, even without major cellular and molecular responses that define the missing tissue response.

RESULTS

follistatin Is Required for Regeneration Only after Complete Head Amputation

To test the requirement for *follistatin* in planarian regeneration broadly, we inflicted a series of injuries that removed varying amounts of tissue after inhibition of *follistatin* by RNAi. Eye resection does not induce a missing tissue response (LoCascio et al., 2017); therefore, eye regeneration following resection was anticipated to occur in *follistatin* RNAi animals. Indeed, all *follistatin* RNAi animals regenerated missing eyes by day 20 after surgery (Figure 1A). Next, we tested larger injuries that removed different types of tissue and that were anticipated to elicit a missing tissue response (Wenemoser and Reddien, 2010; LoCascio et al., 2017). Unexpectedly, almost all *follistatin* RNAi animals subjected to pharynx resections, removal of tissue wedges from the head, sagittal amputations, or removal of posterior tissue regenerated by day 20 after surgery (Figure 1A). A variety of differentiated cell types removed by each of these injury types were regenerated in proper patterns by day 20 post amputation (Figure 1A). In fact, the only tested condition under which *follistatin* RNAi animals failed to regenerate was at anterior-facing wounds (Figure 1A).

The Requirement for *follistatin* in Head Regeneration Is Specific to the Injury Location on the Anterior-Posterior Axis

The requirement of *follistatin* specifically for head regeneration was puzzling. Given that *follistatin* RNAi animals were able to replace anterior cell types after removal of tissue wedges from the head (Figure 1A), we reasoned that there was not a defect in the capacity to make anterior tissue but rather an inability to initiate head regeneration at certain wounds. We therefore assessed whether the position of amputation along the anterior-posterior (AP) axis affects the head regeneration outcome after *follistatin* RNAi. At amputation planes immediately anterior to the base of the pharynx, 0% of *follistatin* RNAi animals regenerated a head (n = 0/30), as expected (Gaviño et al., 2013; Roberts-Galbraith and Newmark, 2013). Following amputation performed slightly anterior to this location, however, 16.1% of *follistatin* RNAi animals regenerated heads (n = 5/31) (Figure 1B). In fact, with each progressively anterior amputation, a larger fraction of animals successfully regenerated a head. At an amputation plane immediately posterior to the auricles (AP1), a location posterior to the brain demarcating the head, 100% of animals regenerated heads (n = 36/36) (Figures 1B and S1A). Amputation at AP1 removes most specialized structures in the head, including the anterior pole, a structure known to act as an organizer for head tissue (Scimone et al., 2014; Vásquez-Doorman and Petersen, 2014; Vogg et al., 2014; Oderberg et al., 2017) (Figures S1A and S1B). Nonetheless, these *follistatin* RNAi fragments regenerated heads without detectable abnormalities, as evidenced by the presence of eyes and a variety of neuronal cell types by day 20 post amputation and successful formation of the anterior pole (Figure 1B). We determined that regeneration at AP1 was not a consequence of RNAi efficacy declining over time. *follistatin* inhibition levels remained comparable from day 0 to day 14 post amputation at AP1 without further delivery of double-stranded (ds)RNA (Figure S1C). In an additional experiment, regeneration at AP1 occurred despite continual injection of *follistatin* dsRNA up to 14 days post injury, which also showed a consistent *follistatin* inhibition level throughout regeneration (Figure S1D). Finally, 100% of *follistatin* RNAi animals that successfully regenerated after amputation at AP1 failed to regenerate heads when subsequently amputated in the tail without further delivery of *follistatin* dsRNA (Figure S1E). These results suggest that the requirement of *follistatin* in head regeneration is dependent upon the location of injury along the AP axis.

follistatin Is Required for the Missing Tissue Response at Multiple Injuries

Prior work has shown that *follistatin* is required for the missing tissue response at anterior-facing amputations in tail fragments (Gaviño et al., 2013). The results described above raised the question of whether *follistatin* is required for the missing tissue response specifically at anterior-facing wounds made in the posterior, with this requirement explaining the head regeneration failure phenotype after this injury. To address this question, we examined the missing tissue response at diverse wound types after *follistatin* RNAi by assessing its three hallmarks: the second peak in proliferation at wounds, sustained expression of wound-induced genes, and the animal-wide increase in apoptosis 72 hr post injury. We found that at posterior-facing wounds and at wounds associated with the removal of a wedge of tissue from

Figure 1. *follistatin* Is Required for Regeneration Only after Complete Head Amputation in the Posterior

(A) *follistatin* is only required for head regeneration. For each surgery: top: live images 20 days after surgery; bottom: fluorescence *in situ* hybridization (FISH) for differentiated tissue markers 20 days after surgery. *opsin*, photoreceptor neurons (green, yellow); *grh-1*, pharynx neurons (magenta); NB.22.1e, dorsal-ventral (DV) boundary, mouth and esophagus (yellow); *cintillo*, sensory neurons (magenta); *gad*, GABAergic neurons (magenta); *notum*, anterior pole (magenta); *wnt1*, posterior pole (magenta). Arrowheads indicate lack of regeneration. Two independent experiments. dpa, days post amputation.

(B) The requirement for *follistatin* in head regeneration diminishes at amputations made at serially anterior locations along the anterior-posterier (AP) axis. "n" describes the number of animals that look like the representative image. % head regeneration is provided in yellow. Bottom: FISH for differentiated tissue markers *notum*, *cintillo*, *gad* pool (anterior pole, sensory neurons, GABAergic neurons; magenta), and *opsin* (photoreceptor neurons; green) at 20 dpa (dorsal view). Two independent experiments.

Scale bars, 200 μm. See also Figure S1.

the head, the second peak in mitotic cell numbers at the wound was significantly reduced after *follistatin* RNAi (Figures 2A–2C). After tissue wedge removal from the head, proliferation near the wound in *follistatin* RNAi animals was comparable to day 0 from day 2 to day 14 post injury despite eye regeneration having occurred by this time point, indicating regeneration could occur with no detectable proliferative response (Figures 2B and S2A). Mitotic numbers were comparable in uninjured *follistatin* and control RNAi animals, suggesting normal levels of proliferation exist during homeostatic tissue turnover (Figures S2B and S2C). Second, the expression levels of *inhibin-1* and *runt-1* (Wenemoser et al., 2012) were reduced at posterior-facing wounds 24–48 hr post tail amputation in *follistatin* RNAi animals (Figures 2D and S2D). Finally, TUNEL$^+$ cell numbers were significantly reduced in *follistatin* RNAi head fragments 72 hr post injury, whereas TUNEL$^+$ cell numbers at 0 hr post injury were comparable to control RNAi animals (Figures 2E and 2F). These data indicate that *follistatin* is required for multiple components of the missing tissue response at diverse wounds, rather than just at anterior-facing wounds.

As described above, *follistatin* RNAi animals can regenerate heads after amputation at AP1 (Figure 1B). We examined the missing tissue response at this injury and found that *follistatin* RNAi animals displayed reduced wound-induced gene expression at 24 hr post injury, no detectable second mitotic peak, and no detectable elevation in apoptosis levels 72 hr after wounding (Figures 2G–2I). In fact, levels of mitosis and apoptosis in regenerating *follistatin* RNAi animals at AP1 were comparable to levels at 0 hr after injury from day 2 through day 10 post amputation, despite successful regeneration of eyes by 10 days post injury. Therefore, regeneration occurred despite no detectable missing tissue response during the course of regeneration from this injury (Figures 2H–2J). These findings together indicate that the missing tissue response is not required for regeneration following a large array of injury types, including small injuries such as eye resection, large injuries such as removal of the posterior half (or more) of the body, and injuries that remove the head.

Regeneration Occurs with a Defective Missing Tissue Response, but at a Slower Rate

Although *follistatin* RNAi animals were able to fully regenerate from multiple injury types, they formed very small blastemas and appeared to replace tissue slower than did controls (Figure 3A). To test this possibility, we used multiple differentiated tissue markers to assess the rate of tissue formation after *follistatin* inhibition and various amputations. In the case of tail amputation, we found that by day 7 post amputation, *follistatin* RNAi animals, unlike controls, had not regenerated the posterior zone of marginal adhesive gland cells (*mag-1*$^+$) and had accumulated mouth cells at the wound face but not yet formed a defined mouth (NB.22.1e$^+$) (Figure 3B). In addition, when we tracked the appearance of pharyngeal tissue over time, using a marker for neurons located at the pharynx tip (Collins et al., 2010), we found that *follistatin* RNAi animals regenerating the posterior half of their bodies had significantly smaller pharynges compared to controls between day 4 and day 10 post amputation (Figures 3B and 3C). However, by day 20 after injury, the posterior zone of marginal adhesive gland cells, the mouth, and the pharynx were completely formed in *follistatin* RNAi animals (Figure S3A).

Regeneration also involves the replacement of lost positional information. Specifically, expression domains of patterning genes (PCGs) return. Some of these expression changes occur in existing muscle cells at wounds and some occur in newly produced muscle cells (Witchley et al., 2013). At 72 hr post injury, posterior-facing wounds begin to form a posterior pole, a group of muscle cells that accumulate near the midline at the posterior tail tip and express the gene *wnt1* (Petersen and Reddien, 2009). In *follistatin* RNAi head fragments, *wnt1*$^+$ cells near the midline of the animal were present at 72 hr but had not yet coalesced into a pole, whereas coalesced poles were present in control animals (Figure 3D). The gene *wntP-2* (sometimes referred to as *wnt11-5*; Gurley et al., 2010) is expressed in a broad posterior-to-anterior transcriptional gradient in muscle and is detectably upregulated at posterior-facing wounds ~30 hr following amputation (Petersen and Reddien, 2009). *wntP-2* was expressed at posterior-facing wounds of *follistatin* RNAi animals, but its expression at 3–5 days post amputation was lower than in controls (Figure 3E) (Gaviño et al., 2013). Regeneration of the expression domains of several posteriorly expressed PCGs is dependent on new cell formation (neoblast proliferation) (Gurley et al., 2010). Regeneration of these expression domains was delayed in *follistatin* RNAi animals (Figure 3E). These data suggest that re-establishment of posterior patterning information can occur with a defective missing tissue response; however, it proceeds slowly. Because regenerative patterning involves both changes in pre-existing muscle cells and new muscle cell production, the slower pace of PCG expression re-establishment is consistent with the lower rate of proliferation in *follistatin* RNAi animals during regeneration.

Similar to the case of posterior amputation, regeneration after amputation of *follistatin* RNAi animals at AP1 occurred despite appreciably reduced blastema size (Figure 4A). Formation of both tissue-specific progenitors and differentiated structures occurred slowly at this injury. Between 2 and 5 days post amputation at AP1, *ovo*$^+$ eye progenitors were fewer in *follistatin* RNAi animals than in controls (Figure S4A) and, at day 7 post amputation, *follistatin* RNAi animals had significantly fewer *cintillo*$^+$ sensory neurons (Figures 4B and 4C), *opsin*$^+$ photoreceptor neurons (Figures 4B and 4D), and *gad*$^+$ GABAergic neurons (Figure S4B).

We also examined the re-setting of positional information after amputation at different AP locations in *follistatin* RNAi animals. *follistatin* RNAi tail fragments obtained by amputation below the pharynx did not form an anterior pole or express anterior PCGs that depend on new muscle cell formation for their expression during regeneration (Figures 4E and S4C) (Roberts-Galbraith and Newmark, 2013). Tail fragments also did not perform patterning steps that occur in existing muscle cells, such as re-scaling the expression domain of the posterior PCG *wntP-2* (Gaviño et al., 2013) and expressing the anterior PCG *wnt-2* (Figure S4C). Posterior fragments obtained by amputation at an intermediate location, AP2, expressed *notum* and *sFRP-1* and formed photoreceptor neurons in ~50% of fragments (Figure S4D). By contrast, all *follistatin* RNAi animals amputated at

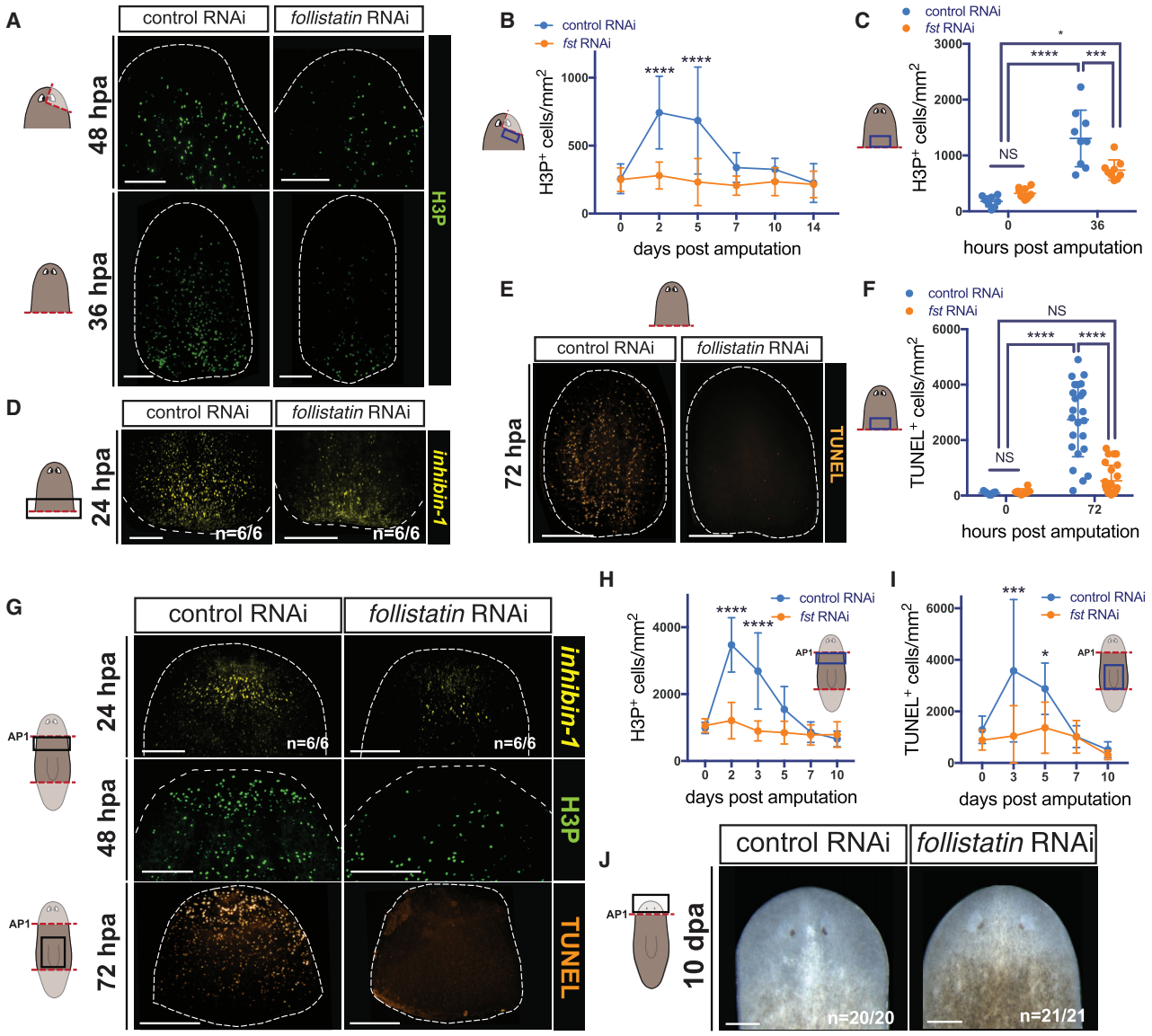

Figure 2. *follistatin* Is Required for the Missing Tissue Response at Multiple Injury Types

(A) *follistatin* is required for the second mitotic peak after tail amputation and removal of tissue wedges from the head. Phospho-histone H3 (H3P) antibody labeling to mark mitotic cells (green) after the indicated injury at the specified time point (ventral view). Two independent experiments.

(B) Graph displays the number of $H3P^+$ cells counted in the region marked by the blue box at the indicated times after head wedge removal. ****$p < 0.0001$. $n > 8$ per time point; $n > 30$, 2 dpa; $n > 20$, 0 hours post amputation (hpa).

(C) Graph displays the number of $H3P^+$ cells counted in the region marked by the blue box at 0 hpa and 36 hpa. ****$p < 0.001$, ***$p < 0.001$, *$p < 0.05$.

(D) *follistatin* is required for perduring wound-induced gene expression at posterior-facing wounds. FISH for the wound-induced gene *inhibin-1* (yellow) at 24 hpa in regenerating head fragments (dorsal view). Black box indicates the region shown. Two independent experiments.

(E) *follistatin* is required for the 72-hr wave of apoptosis after tail amputation. TUNEL marked cells undergoing apoptosis (orange) at 72 hpa in regenerating head fragments (ventral view). Four independent experiments.

(F) Graph displays the number of $TUNEL^+$ cells counted in regenerating head fragments at the indicated time points. ****$p < 0.0001$.

(G) *follistatin* is required for the missing tissue response after AP1 amputation. FISH for the wound-induced gene *inhibin-1* (yellow) at 24 hpa (dorsal view). H3P antibody labeling to mark mitotic cells (green) at 48 hpa (ventral view). TUNEL marked apoptotic cells (orange) in pharynges at 72 hpa. Black box indicates the region shown. Two independent experiments.

(H) Graph displays the number of $H3P^+$ cells counted near the wound, indicated by the blue box. Anterior regeneration at AP1 displayed a higher second mitotic peak than posterior regeneration in control RNAi animals. $n \geq 8$ for each time point. $n > 20$, 0 hpa; $n > 25$, 2 dpa. ****$p < 0.0001$.

(I) Graph displays the number of $TUNEL^+$ cells counted in the pharynges of regenerating trunks indicated by the blue box. $n \geq 6$ for each time point. ***$p < 0.001$, *$p < 0.05$.

(J) Live images of head regeneration outcome 10 dpa at AP1 after *follistatin* RNAi.

Scale bars, 200 μm. Error bars represent mean ± SD. NS indicates no significant difference. See also Figure S2.

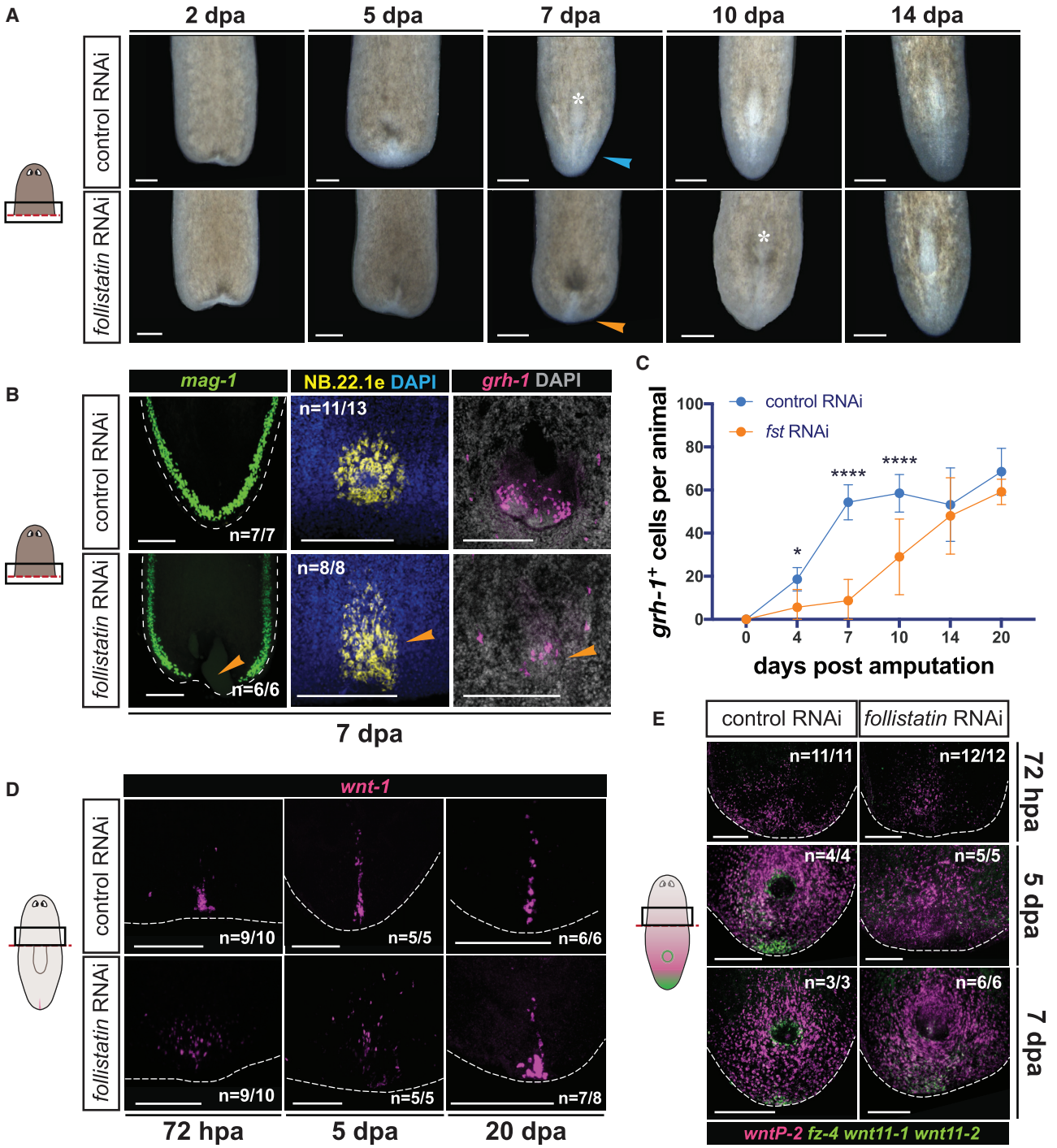

Figure 3. Posterior Regeneration Occurs with a Defective Missing Tissue Response, but at a Slower Rate

(A) *follistatin* RNAi head fragments regenerate slowly with small blastemas. Live images at the indicated time points post amputation. Asterisks mark a newly formed pharynx. Arrowheads indicate a blastema.

(B) Multiple differentiated tissue structures appear small or absent at 7 days post tail amputation after *follistatin* RNAi. FISH to mark marginal adhesive gland cells (*mag-1*$^+$, green), the mouth (NB.22.1e$^+$, yellow), and pharyngeal neurons (*grh-1*, magenta) (ventral view). Black box indicates the region shown. Two independent experiments.

(C) *follistatin* RNAi animals regenerate pharynges slowly and are indistinguishable from controls by 14 days post tail amputation. Graph indicates the number of *grh-1*$^+$ cells counted per animal at the specified time points post tail amputation. Data are plotted as mean ± SD. n > 8 for each time point. ****p < 0.0001, *p < 0.05.

(legend continued on next page)

AP1 re-established anterior patterning information, but slowly, with reduced expression of the anterior PCG *ndl-5* and delayed coalescence of the anterior pole between days 3 and 5 post injury (Figures 4F and S4E).

Taken together, these findings support a model in which the missing tissue response accelerates patterning and tissue replacement but is not required to bring about regeneration of any missing body part, including a head, following a large diversity of injury classes.

follistatin Inhibits Early Wound-Induced *wnt1* Expression at All Injuries

Why is *follistatin* required for head regeneration at amputations in the trunk and posterior of animals, but not required for head regeneration after amputation in the anterior? Wnt signaling is known to be important for re-setting positional information and for replacing missing body parts after injury to the AP axis (Gurley et al., 2008; Iglesias et al., 2008; Petersen and Reddien, 2008, 2009, 2011; Adell et al., 2009). Planarians maintain a gradient of Wnt signaling activity along their AP axis during homeostasis and re-establish this gradient during regeneration (Gurley et al., 2008, 2010; Petersen and Reddien, 2008, 2009; Adell et al., 2009; Sureda-Gómez et al., 2016; Stückemann et al., 2017). Soon after wounding, both anterior-facing and posterior-facing wounds (indeed, essentially all wounds) express the *wnt1* gene (Petersen and Reddien, 2009). Another wound-induced gene, *notum*, is preferentially induced at anterior-facing wounds over posterior-facing wounds (Petersen and Reddien, 2011; Wurtzel et al., 2015). *notum* encodes a broadly conserved deacylase that inhibits the action of Wnt ligands (Kakugawa et al., 2015; Zhang et al., 2015). Both *wnt1* and *notum* are wound induced in muscle cells (Witchley et al., 2013), and within 24 hr post amputation a low-Wnt signaling environment is established at anterior-facing amputations (head generating) and a high-Wnt environment is established at posterior-facing amputations (tail generating) (Stückemann et al., 2017). *notum* RNAi leads to regeneration of tails instead of heads at anterior-facing wounds (Petersen and Reddien, 2011), and *wnt1* RNAi leads to either failed tail regeneration or the regeneration of heads instead of tails at posterior-facing wounds (Adell et al., 2009; Petersen and Reddien, 2009).

Given the importance of Wnt signaling in the decision to make a head or tail, we asked whether *follistatin* might impact wound-regulated Wnt signaling to mediate its role in head regeneration. We assessed the expression of *notum* and *wnt1* early after wounding in regenerating tail fragments, amputated below the pharynx. Wound-induced *notum* expression was normal between 6 and 24 hr post amputation (Figures 5A, S5A, and S5B); however, the formation of a *notum*$^{+}$ anterior pole at later time points did not occur in *follistatin* RNAi tail fragments, as previously reported (Roberts-Galbraith and Newmark, 2013) (Figure S5A). Wound-induced *wnt1* expression, however, was robustly higher compared to controls in *follistatin* RNAi tail fragments between 6 and 12 hr post amputation, before returning to normal levels by 24 hr after injury (Figures 5B, 5C, and S5A). Elevated wound-induced expression of *wnt1* after *follistatin* RNAi was observed at all wound types tested, including wounds that did not remove substantial tissue, and occurred in muscle cells, which is the normal site of wound-induced *wnt1* expression (Figures 5B and S5C). This effect on wound-induced gene expression was specific to *wnt1*, with multiple other wound-induced genes, including those induced in muscle, not affected by *follistatin* RNAi at 6 hr post injury (Scimone et al., 2017) (Figures 5A and 5C). We also did not observe any changes in the expression of β-*catenin-1*-sensitive genes during homeostasis in *follistatin* RNAi animals, suggesting that homeostatic Wnt signaling levels were unaffected (Figure S5D). RNAi of *activin-1*, a gene encoding an Activin-like TGF-β-family signliang ligand, is known to suppress the head regneration defect of *follistatin* RNAi tail fragments (Gaviño et al., 2013; Roberts-Galbraith and Newmark, 2013). We found that increased *wnt1* expression at wounds after follistatin RNAi was dependent on *activin-1*, (Figures 5D, S5E, and S5F), but *activin-1* RNAi had no effect on *notum* expression at wounds (Figure S5G). This suggests that *follistatin* is required to inhibit the expression levels of wound-induced *wnt1* in an Activin-dependent manner.

Inhibition of *wnt1* Suppresses the Head Regeneration Defect of *follistatin* RNAi Animals

Defective *follistatin*-mediated inhibition of the Wnt-ligand-encoding *wnt1* gene could explain why head amputations made at posterior locations fail to regenerate. The planarian posterior has inherently high Wnt signaling during homeostasis (Petersen and Reddien, 2008; Adell et al., 2009; Gurley et al., 2010; Sureda-Gómez et al., 2016; Stückemann et al., 2017), and anterior-facing wounds in the posterior must generate a low-Wnt environment for head regeneration to occur. Increased wound-induced *wnt1*, in what is naturally a high-Wnt signaling environment, could therefore lead to head regeneration failure in *follistatin* RNAi animals. Conversely, many genes encoding Wnt inhibitors, including *notum* and *sFRPs*, are expressed in the low-Wnt anterior region of the animal during homeostasis (Gurley et al., 2008, 2010; Petersen and Reddien, 2008, 2011). This low-Wnt anterior environment might favor head regeneration even in the presence of elevated levels of *wnt1* at the wound face.

To determine whether the elevated level of *wnt1* expression in *follistatin* RNAi animals is required for the head regeneration defect observed, we simultaneously inhibited *follistatin* and *wnt1* and assessed regeneration in tail fragments. Whereas almost all tails treated with *follistatin*; control dsRNA (36/37) did not regenerate a head, 32/49 tails treated with *wnt1; follistatin* dsRNA successfully regenerated, despite similar *follistatin*

(D) The posterior pole forms slowly in regenerating head fragments after *follistatin* RNAi. FISH for *wnt1* to mark the posterior pole (magenta). Dorsal view. Black box indicates the region shown. Two independent experiments.

(E) Posterior patterning occurs slowly in regenerating head fragments after *follistatin* RNAi. FISH for posterior patterning genes *wntP-2* (magenta) and *fz-4*, *wnt11-1*, and *wnt11-2* pool (green) at the indicated time points after tail amputation (ventral view). Black box indicates the region shown. Two independent experiments. Scale bars, 200 μm. See also Figure S3.

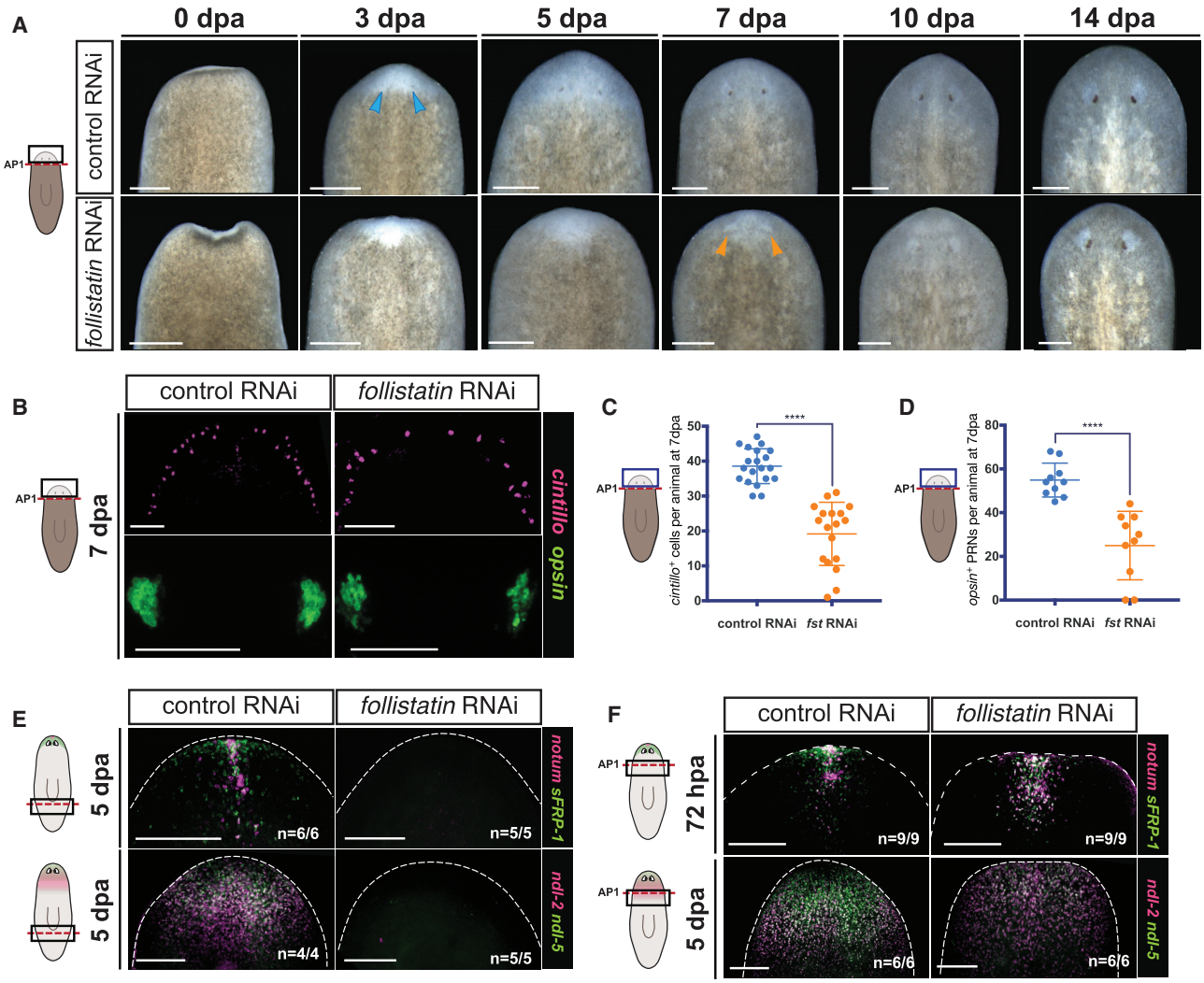

Figure 4. Head Regeneration at AP1 Occurs in the Absence of a Detectable Missing Tissue Response, but at a Slower Rate

(A) *follistatin* RNAi animals regenerate heads slowly after amputation at AP1. Live images at the indicated time points post amputation. Arrowheads indicate the first appearance of eyes.

(B) Differentiated anterior tissues are less developed than in controls 7 days post AP1 amputation in *follistatin* RNAi animals. FISH for differentiated tissue markers *opsin* (photoreceptor neurons, green; dorsal view) and *cintillo* (sensory neurons, magenta; ventral view). Black box indicates the region shown. Two independent experiments.

(C) Number of *cintillo*$^+$ sensory neurons at 7 dpa. Blue box indicates the region quantified. ****$p < 0.0001$.

(D) Number of *opsin*$^+$ photoreceptor neurons at 7 dpa. Blue box indicates the region quantified. ****$p < 0.0001$.

(E) Anterior patterning and pole formation do not occur after amputation below the pharynx in *follistatin* RNAi animals. Top: FISH for *notum* (magenta) and *sFRP-1* (green) at 5 dpa (ventral view). Bottom: FISH for *ndl-2* (magenta) and *ndl-5* (green) at 5 dpa (ventral view). Black box indicates the region shown. Two independent experiments.

(F) Anterior patterning and pole formation occur slowly after amputation at AP1 in *follistatin* RNAi animals. Top: FISH for *notum* (magenta) and *sFRP-1* (green) at 72 hpa (ventral view). Bottom: FISH for *ndl-2* (magenta) and *ndl-5* (green) at 5 dpa (ventral view). Black box indicates the region shown. Two independent experiments.

Scale bars, 200 μm (A, E, and F) and 100 μm (B). Error bars represent mean ± SD. See also Figure S4.

expression-level reduction in both conditions (Figures 6A and S6A). The regenerated heads of *wnt1; follistatin* double-RNAi animals had no observed morphological abnormalities (Figures 6A and S6B). We performed a similar experiment by simultaneous inhibition of *follistatin* and β-*catenin-1*, the intracellular effector of canonical Wnt signaling. β-*catenin-1* RNAi also rescued the head regeneration failure phenotype of *follistatin* RNAi animals (Figures S6C and S6D). In addition, we performed double RNAi of *myoD* and β-*catenin-1*. *myoD* is required for wound-induced expression of *follistatin* but does not affect wound-induced *wnt1* expression, and *myoD* RNAi leads to regeneration failure (Scimone et al., 2017). We found that

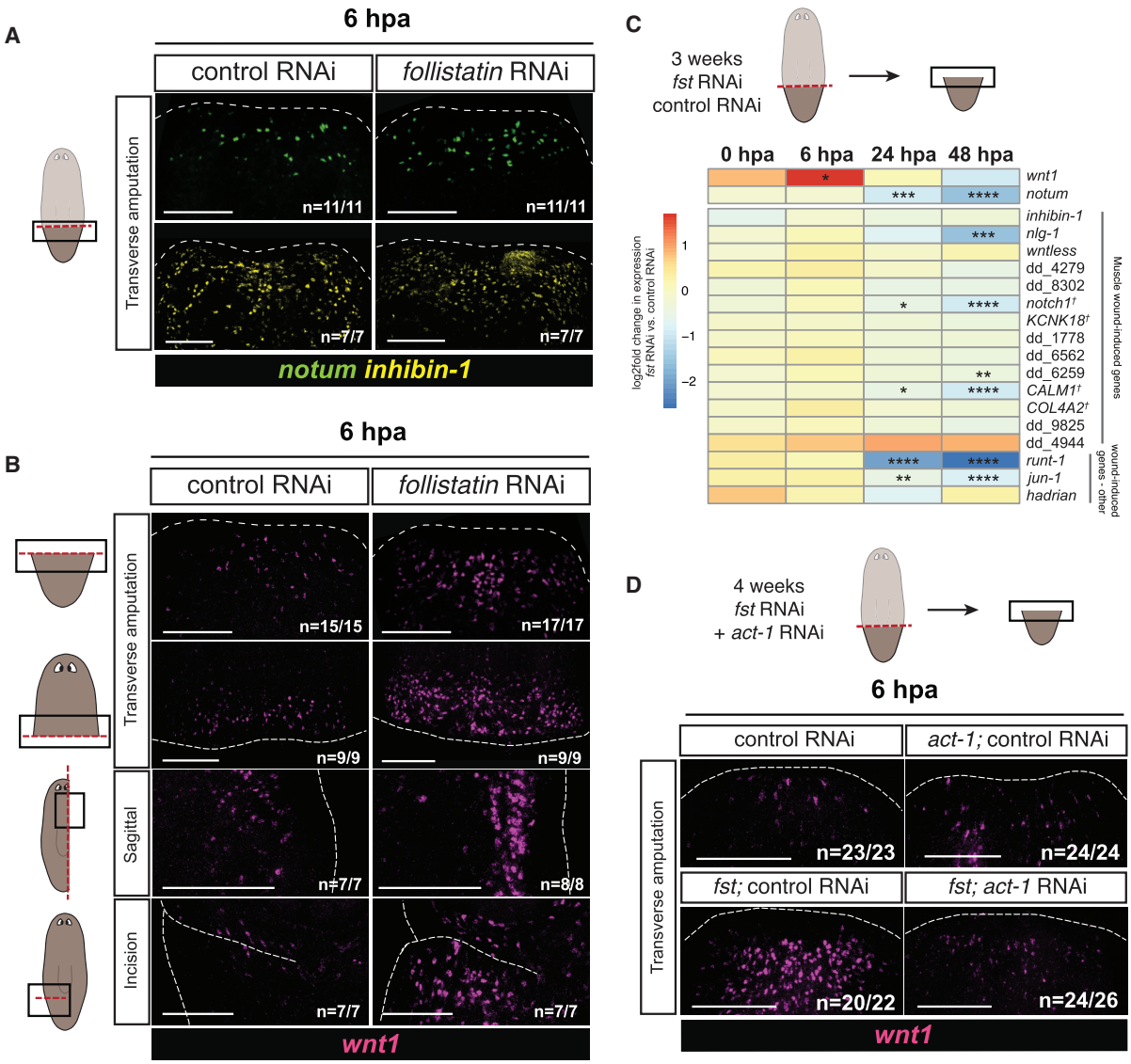

Figure 5. *follistatin* Inhibits Wound-Induced Expression Levels of *wnt1* at Diverse Injuries

(A) Expression levels of wound-induced *notum* and *inhibin-1* are normal after *follistatin* RNAi. FISH for *notum* (green) and *inhibin-1* (yellow) at 6 hpa in regenerating tail fragments (ventral view). Black box indicates the region shown. Two independent experiments.

(B) *follistatin* is required to inhibit *wnt1* expression early after wounding at many injuries. FISH for *wnt1* (magenta) at 6 hr after the indicated surgeries (ventral view). Black box indicates the region shown. Two independent experiments.

(C) *follistatin* is not required to inhibit expression of other wound-induced genes at 6 hpa. Heatmap depicts RNA sequencing (RNA-seq) data of anterior-facing wounds collected from *follistatin* RNAi and control RNAi tail fragments (Scimone et al., 2017). Data are presented as $\log_2$ fold change in gene expression between *follistatin* RNAi and control RNAi at the indicated time points post amputation. *$p_{adj} < 0.05$, **$p_{adj} < 0.01$, ***$p_{adj} < 0.001$, ****$p_{adj} < 0.0001$. †Best human BLAST hits.

(D) *follistatin*-mediated inhibition of *wnt1* is dependent on *activin-1*. Top: feeding regimen for RNAi. Bottom: FISH for *wnt1* (magenta) at 6 hpa in each RNAi condition. Black box indicates the region shown. Two independent experiments.

Scale bars, 200 μm. See also Figure S5.

myoD; β-catenin-1 RNAi tails were also able to regenerate despite reduced expression of *follistatin* at wounds after 1 week of *myoD* RNAi (Figures S6E and S6F). Previous work has shown that *myoD; β-catenin-1* RNAi tails do not regenerate heads after 3 weeks of *myoD* RNAi (Scimone et al., 2017). *myoD* is required for the specification of longitudinal muscle fibers, suggesting that after 3 weeks of dsRNA treatment a larger reduction in longitudinal fibers, and further loss of any attendant additional roles of these fibers, results in the failed regeneration of *myoD; β-catenin-1* double-RNAi animals. These data indicate that inhibition of Wnt signaling can rescue the head regeneration defect caused by RNAi of *follistatin*.

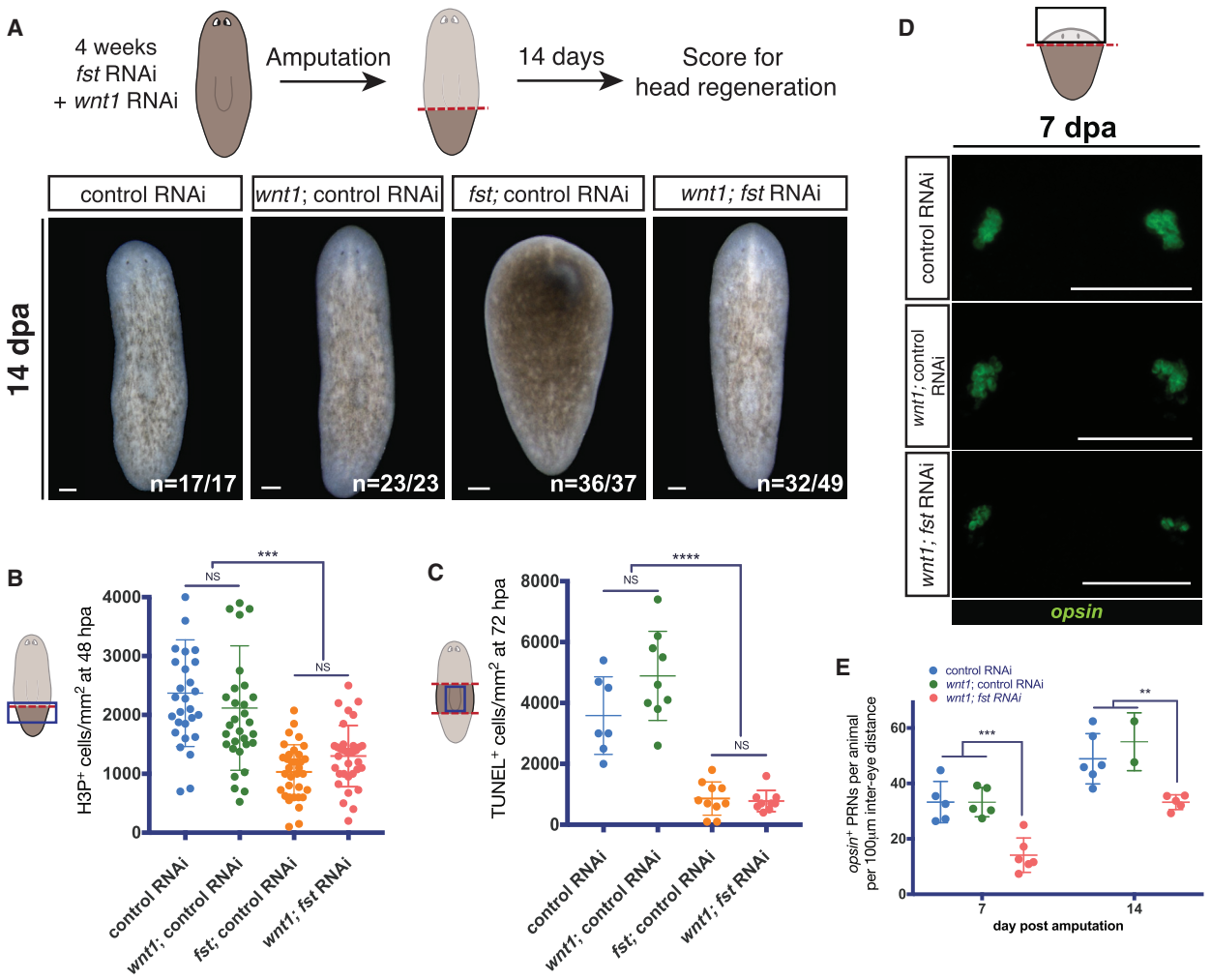

Figure 6. *wnt1* Inhibition Restores Head Regeneration after *follistatin* RNAi Despite a Defective Missing Tissue Response

(A) *wnt1* RNAi suppresses the head regeneration defect after *follistatin* RNAi. Top: feeding regimen for RNAi. Bottom: live images of tail fragments at 14 dpa. Two independent experiments.

(B) Simultaneous inhibition of *wnt1* and *follistatin* does not restore the secondary mitotic peak in regenerating tail fragments. Graph displays the number of $H3P^+$ cells counted in the region indicated by the blue box at 48 hpa for each RNAi condition. ***$p < 0.001$. Three independent experiments.

(C) Inhibition of *wnt1* does not suppress the defect in the 72-hpa apoptotic wave caused by *follistatin* RNAi. Graph: $TUNEL^+$ cell numbers per pharynx (indicated by the blue box) at 72 hpa, in regenerating trunks, for each RNAi condition. ****$p < 0.0001$. Three independent experiments.

(D) *wnt1; follistatin* double-RNAi animals regenerate eyes slowly compared to controls. FISH for *opsin* (photoreceptor neurons, green) at 7 dpa (dorsal view). Black box indicates the region shown.

(E) Graph displays the number of $opsin^+$ photoreceptor neurons counted per animal for each RNAi condition at the specified time points.

Scale bars, 200 μm (A) and 100 μm (D). Error bars represent mean ± SD. NS indicates no significant difference. See also Figures S6 and S7.

Head Regeneration from the Posterior in *wnt1; follistatin* Double-RNAi Animals Occurs Despite a Diminished Missing Tissue Response

We considered the possibilities that inhibition of wound-induced *wnt1* by *follistatin* initiates the missing tissue response or that *follistatin* separately regulates *wnt1* expression and the missing tissue response. To distinguish between these two possibilities, we tested whether *wnt1* inhibition suppresses the missing tissue response defect in *follistatin* RNAi tail fragments. *wnt1; follistatin* double-RNAi tail fragments still showed a diminished second mitotic peak at 48 hr post amputation (Figure 6B) and reduced cell death at 72 hr after injury (Figure 6C), suggesting that the missing tissue response defect of *follistatin* RNAi animals had not been suppressed by *wnt1* RNAi. *wnt1; follistatin* double-RNAi tail fragments initiated anterior pole formation at 72 hr post injury, suggesting these animals could re-set positional information (Figure S7A). Furthermore, regeneration of multiple differentiated tissues, including the eyes, brain, and pharynx, occurred in these fragments, but slowly compared to *wnt1;* control RNAi and control RNAi tails (Figures 6D, 6E, and S7B–S7D). These findings indicate that head regeneration in the posterior does not require a normal missing tissue

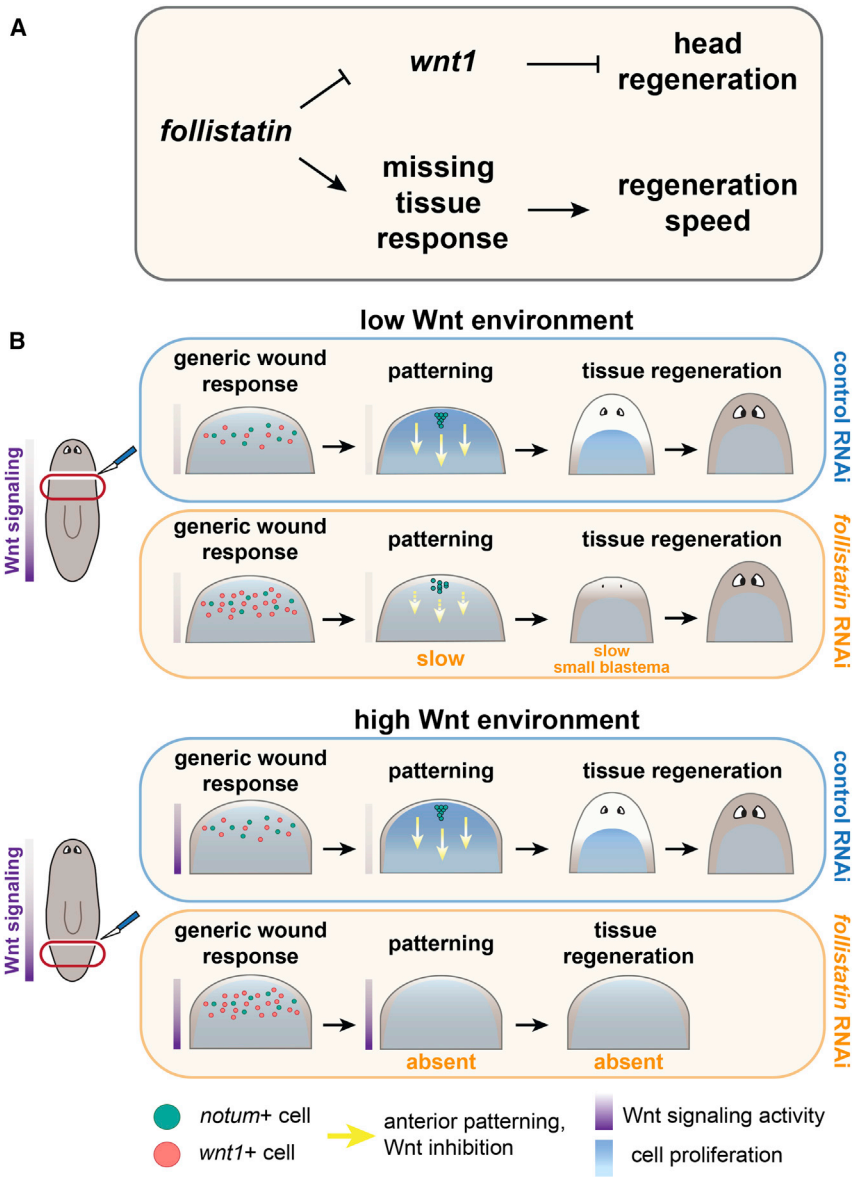

Figure 7. Model for the Roles of the Missing Tissue Response and *follistatin* in Regeneration

(A) Model for the role of *follistatin* in planarian regeneration.

(B) Schematic depicting head regeneration after *follistatin* RNAi in high- (posterior) and low- (anterior) Wnt signaling environments. Head regeneration can occur in a low-Wnt signaling environment even in the absence of a detectable missing tissue response, but at reduced speed. Amputation in a high-Wnt signaling environment requires appropriate regulation of wound-induced Wnt signaling. Elevated wound-induced *wnt1* expression after *follistatin* RNAi causes regeneration of anterior patterning information and anterior tissue formation to fail.

response, and suggest that *follistatin* separately regulates wound-induced Wnt signaling and the missing tissue response (Figure 7).

DISCUSSION

Identifying the cellular and molecular processes that are required for regeneration is a fundamental problem in understanding adult wound repair. In many regenerative organisms a large array of cellular responses are triggered at major injuries, prominently including elevated cell proliferation (Poleo et al., 2001; Nechiporuk and Keating, 2002; Chera et al., 2009; Poss, 2010; Tanaka and Reddien, 2011; Srivastava et al., 2014). For instance, similar to the case of planarian regeneration, limb regeneration in axolotls involves phases of gene expression and sustained cell proliferation specifically associated with blastema formation after amputation and absent in lateral wounds that do not remove substantial tissue (Knapp et al., 2013). However, which cellular processes are required for tissue regeneration to occur across animals remains an open question. Our findings suggest that prominent cellular and molecular responses unique to substantial tissue loss that are hallmarks of regeneration in planarians, collectively called the missing tissue or regenerative response, are not required for regeneration. We determined that regeneration from all injury types tested can occur with a defective missing tissue response, although at a significantly reduced speed. We propose that the missing tissue response functions to accelerate, rather than to bring about, regeneration (Figure 7).

This leads to the question of what is fundamentally required to bring about regeneration. All new cell production in planarian regeneration requires neoblasts, and neoblasts constantly divide and produce fate-specified progenitors during tissue turnover (Reddien, 2013; Zhu and Pearson, 2016). Neoblasts are therefore required for regeneration (Bardeen and Baetjer, 1904; Dubois, 1949; Reddien et al., 2005; Baguñà, 2012). Data suggest that re-setting of positional information is a critical component of regeneration. Regeneration of the AP axis after amputation begins with the regulation of Wnt signaling by generic wound signaling, followed by anterior pole formation, re-establishment of positional information, and tissue replacement. We found that *follistatin* affects the earliest of these steps through inhibition of the level of wound-induced *wnt1* expression. This increase in *wnt1* expression at wounds was associated with failure to re-set positional information and an inability to regenerate anterior tissue at amputations in the posterior, where homeostatic Wnt signaling levels are high. Tail fragments that fail to regenerate a head continue to turn over existing tissue, similar to the phenotype of *myoD* RNAi animals, suggesting

follistatin RNAi amputated tail fragments have an inability to generate any tissue that is missing (Gaviño et al., 2013; Scimone et al., 2017). Blocking generic wound-induced gene expression with an inhibitor to Erk signaling also blocks regeneration (Owlarn et al., 2017). These data suggest generic wound signaling, prominently involving *wnt1* and *notum*, is required for re-setting positional information and that this can be required for regeneration. By contrast, all other wound types from which *follistatin* RNAi animals could regenerate were able to re-pattern tissue after injury but did so slowly. In addition, inhibition of *wnt1* was sufficient to rescue patterning and tissue regeneration in *follistatin* RNAi tail fragments. These data suggest that the re-setting of positional information by wound regulation of Wnt signaling could mediate regeneration even without a detectable missing tissue response.

In some conditions, such as following RNAi of *patched*, *notum*, or *APC*, increased Wnt signaling at anterior-facing wounds can result in ectopic tail regeneration rather than failed regeneration (Gurley et al., 2008; Rink et al., 2009; Yazawa et al., 2009; Petersen and Reddien, 2011). In the case of *follistatin* RNAi, the significantly reduced missing tissue response at wounds is associated with a slow rate of positional information re-setting. This might not allow enough time for induction of an ectopic tail program while *wnt1* is overexpressed. *follistatin* RNAi also differs from these other conditions in that increased *wnt1* expression occurs only between 6 and 12 hours post amputation, whereas it persists up to at least 24 hours post amputation after *patched* RNAi (Rink et al., 2009). Because these *follistatin* RNAi anterior-facing wounds have normal expression levels of wound-induced *notum* up to 24 hours post amputation, this could make ectopic tail formation unlikely at these injuries.

Planarians can regenerate from small injuries, such as eye resection, as an emergent property of homeostatic tissue turnover without elevated cell proliferation (LoCascio et al., 2017). However, major injuries pose additional challenges—in addition to the loss of organs, organ-specific progenitors and the positional information for specifying those progenitors can be lost. A reasonable assumption has been that responses such as increased cell proliferation during blastema formation play a key role in overcoming these challenges. Our findings suggest that this is not the case in planarians. We propose a model in which regenerative re-patterning on the AP axis, induced by regulation of generic wound-induced Wnt signaling, coupled with continuous production of progenitors associated with tissue turnover, can bring about regeneration from diverse wound scenarios. The generic wound response (the *follistatin*-independent response occurring 1 to 6 hr post injury) has been implicated in initiating re-establishment of positional information and regeneration (Petersen and Reddien, 2009, 2011; Owlarn et al., 2017; Scimone et al., 2017). Aspects of the generic wound response could prove to have additional contributions to regeneration. Furthermore, there could prove to exist specific responses to missing tissue injuries that are *follistatin* independent and that contribute to the capacity for regeneration. These will be important targets for continued investigation. Taken together, our results suggest that in the absence of detectable cellular and molecular responses specific to major injuries, regulation of wound-induced Wnt signaling for regenerative re-patterning together with continuous tissue turnover can mediate successful regeneration in essentially any wound context (Figure 7).

STAR★METHODS

Detailed methods are provided in the online version of this paper and include the following:

- KEY RESOURCES TABLE
- CONTACT FOR REAGENT AND RESOURCE SHARING
- EXPERIMENTAL MODEL AND SUBJECT DETAILS
- METHOD DETAILS
  - Double-stranded RNA synthesis for RNAi experiments
  - Double-stranded RNA injections for RNAi
  - Microsurgery
  - Fixation
  - Whole-mount *in situ* hybridizations
  - phospho-Histone H3 labeling
  - TUNEL
  - Quantitative real-time PCR (qRT-PCR)
  - RNA sequencing Analysis
  - Microscopy and image analysis
- QUANTIFICATION AND STATISTICAL ANALYSIS

SUPPLEMENTAL INFORMATION

Supplemental Information includes seven figures and two tables and can be found with this article online at https://doi.org/10.1016/j.celrep.2018.11.004.

ACKNOWLEDGMENTS

We thank the members of the Reddien lab for comments and discussion. We thank Jason Pellettieri and John Dustin for the H3P antibody and TUNEL protocols. We acknowledge support from the NIH (R01GM080639). A.G.T. was supported by the National Science Foundation Graduate Research Fellowship Program. We thank the Eleanor Schwartz Charitable Foundation for support. P.W.R. is an Investigator of the Howard Hughes Medical Institute and an Associate Member of the Broad Institute of Harvard and MIT.

AUTHOR CONTRIBUTIONS

Conceived and designed the experiments, A.G.T., S.R.S., I.M.O., and P.W.R. Performed the experiments, A.G.T., S.R.S., and P.W.R. Analyzed the data, A.G.T., S.R.S., and P.W.R. Wrote the paper, A.G.T. and P.W.R. Revised the paper, A.G.T., S.R.S., I.M.O., and P.W.R.

DECLARATION OF INTERESTS

The authors declare no competing interests.

Received: May 30, 2018
Revised: September 11, 2018
Accepted: October 31, 2018
Published: November 27, 2018

SUPPORTING CITATIONS

The following references appear in the Supplemental Information: Cowles et al. (2013); Lapan and Reddien (2012); Nishimura et al. (2008); Oviedo et al. (2003); Sánchez Alvarado and Newmark, 1999; van Wolfswinkel et al. (2014); Zayas et al. (2010).

REFERENCES

Adell, T., Salò, E., Boutros, M., and Bartscherer, K. (2009). *Smed-Evi/Wntless* is required for beta-catenin-dependent and -independent processes during planarian regeneration. Development *136*, 905–910.

Anders, S., and Huber, W. (2010). Differential expression analysis for sequence count data. Genome Biol. *11*, R106.

Baguñà, J. (1976). Mitosis in the intact and regenerating planarian *Dugesia mediterranea* n.sp. I. Mitotic studies during growth, feeding and starvation. J. Exp. Zool. *195*, 53–64.

Baguñà, J. (2012). The planarian neoblast: the rambling history of its origin and some current black boxes. Int. J. Dev. Biol. *56*, 19–37.

Bardeen, C.R., and Baetjer, F.H. (1904). The inhibitive action of the Roentgen rays on regeneration in planarians. J. Exp. Zool. *1*, 191–195.

Benian, G.M., Kiff, J.E., Neckelmann, N., Moerman, D.G., and Waterston, R.H. (1989). Sequence of an unusually large protein implicated in regulation of myosin activity in *C. elegans*. Nature *342*, 45–50.

Brandl, H., Moon, H., Vila-Farré, M., Liu, S.Y., Henry, I., and Rink, J.C. (2016). PlanMine—a mineable resource of planarian biology and biodiversity. Nucleic Acids Res. *44*, D764–D773.

Chera, S., Ghila, L., Dobretz, K., Wenger, Y., Bauer, C., Buzgariu, W., Martinou, J.C., and Galliot, B. (2009). Apoptotic cells provide an unexpected source of Wnt3 signaling to drive hydra head regeneration. Dev. Cell *17*, 279–289.

Collins, J.J., III, Hou, X., Romanova, E.V., Lambrus, B.G., Miller, C.M., Saberi, A., Sweedler, J.V., and Newmark, P.A. (2010). Genome-wide analyses reveal a role for peptide hormones in planarian germline development. PLoS Biol. *8*, e1000509.

Cowles, M.W., Brown, D.D., Nisperos, S.V., Stanley, B.N., Pearson, B.J., and Zayas, R.M. (2013). Genome-wide analysis of the bHLH gene family in planarians identifies factors required for adult neurogenesis and neuronal regeneration. Development *140*, 4691–4702.

Dubois, F. (1949). Contribution à l'étude de la migration des cellules de régénération chez les *Planaires dulcicoles*. Bull. Biol. Fr. Belg. *83*, 213–283.

Gaviño, M.A., Wenemoser, D., Wang, I.E., and Reddien, P.W. (2013). Tissue absence initiates regeneration through Follistatin-mediated inhibition of Activin signaling. eLife *2*, e00247.

Gurley, K.A., Rink, J.C., and Sánchez Alvarado, A. (2008). Beta-catenin defines head versus tail identity during planarian regeneration and homeostasis. Science *319*, 323–327.

Gurley, K.A., Elliott, S.A., Simakov, O., Schmidt, H.A., Holstein, T.W., and Sánchez Alvarado, A. (2010). Expression of secreted Wnt pathway components reveals unexpected complexity of the planarian amputation response. Dev. Biol. *347*, 24–39.

Iglesias, M., Gomez-Skarmeta, J.L., Saló, E., and Adell, T. (2008). Silencing of *Smed-βcatenin1* generates radial-like hypercephalized planarians. Development *135*, 1215–1221.

Kakugawa, S., Langton, P.F., Zebisch, M., Howell, S., Chang, T.H., Liu, Y., Feizi, T., Bineva, G., O'Reilly, N., Snijders, A.P., et al. (2015). Notum deacylates Wnt proteins to suppress signalling activity. Nature *519*, 187–192.

King, R.S., and Newmark, P.A. (2013). *In situ* hybridization protocol for enhanced detection of gene expression in the planarian *Schmidtea mediterranea*. BMC Dev. Biol. *13*, 8.

Knapp, D., Schulz, H., Rascon, C.A., Volkmer, M., Scholz, J., Nacu, E., Le, M., Novozhilov, S., Tazaki, A., Protze, S., et al. (2013). Comparative transcriptional profiling of the axolotl limb identifies a tripartite regeneration-specific gene program. PLoS ONE *8*, e61352.

Langmead, B., Trapnell, C., Pop, M., and Salzberg, S.L. (2009). Ultrafast and memory-efficient alignment of short DNA sequences to the human genome. Genome Biol. *10*, R25.

Lapan, S.W., and Reddien, P.W. (2012). Transcriptome analysis of the planarian eye identifies *ovo* as a specific regulator of eye regeneration. Cell Rep. *2*, 294–307.

LoCascio, S.A., Lapan, S.W., and Reddien, P.W. (2017). Eye absence does not regulate planarian stem cells during eye regeneration. Dev. Cell *40*, 381–391.e3.

Nechiporuk, A., and Keating, M.T. (2002). A proliferation gradient between proximal and msxb-expressing distal blastema directs zebrafish fin regeneration. Development *129*, 2607–2617.

Nishimura, K., Kitamura, Y., Umesono, Y., Takeuchi, K., Takata, K., Taniguchi, T., and Agata, K. (2008). Identification of glutamic acid decarboxylase gene and distribution of GABAergic nervous system in the planarian *Dugesia japonica*. Neuroscience *153*, 1103–1114.

Oderberg, I.M., Li, D.J., Scimone, M.L., Gaviño, M.A., and Reddien, P.W. (2017). Landmarks in existing tissue at wounds are utilized to generate pattern in regenerating tissue. Curr. Biol. *27*, 733–742.

Oviedo, N.J., Newmark, P.A., and Sánchez Alvarado, A. (2003). Allometric scaling and proportion regulation in the freshwater planarian *Schmidtea mediterranea*. Dev. Dyn. *226*, 326–333.

Owlarn, S., Klenner, F., Schmidt, D., Rabert, F., Tomasso, A., Reuter, H., Mulaw, M.A., Moritz, S., Gentile, L., Weidinger, G., and Bartscherer, K. (2017). Generic wound signals initiate regeneration in missing-tissue contexts. Nat. Commun. *8*, 2282.

Pearson, B.J., Eisenhoffer, G.T., Gurley, K.A., Rink, J.C., Miller, D.E., and Sánchez Alvarado, A. (2009). Formaldehyde-based whole-mount in situ hybridization method for planarians. Dev. Dyn. *238*, 443–450.

Pellettieri, J., Fitzgerald, P., Watanabe, S., Mancuso, J., Green, D.R., and Sánchez Alvarado, A. (2010). Cell death and tissue remodeling in planarian regeneration. Dev. Biol. *338*, 76–85.

Petersen, C.P., and Reddien, P.W. (2008). *Smed-betacatenin-1* is required for anteroposterior blastema polarity in planarian regeneration. Science *319*, 327–330.

Petersen, C.P., and Reddien, P.W. (2009). A wound-induced Wnt expression program controls planarian regeneration polarity. Proc. Natl. Acad. Sci. USA *106*, 17061–17066.

Petersen, C.P., and Reddien, P.W. (2011). Polarized *notum* activation at wounds inhibits Wnt function to promote planarian head regeneration. Science *332*, 852–855.

Poleo, G., Brown, C.W., Laforest, L., and Akimenko, M.A. (2001). Cell proliferation and movement during early fin regeneration in zebrafish. Dev. Dyn. *221*, 380–390.

Poss, K.D. (2010). Advances in understanding tissue regenerative capacity and mechanisms in animals. Nat. Rev. Genet. *11*, 710–722.

Reddien, P.W. (2013). Specialized progenitors and regeneration. Development *140*, 951–957.

Reddien, P.W. (2018). The cellular and molecular basis for planarian regeneration. Cell *175*, 327–345.

Reddien, P.W., Oviedo, N.J., Jennings, J.R., Jenkin, J.C., and Sánchez Alvarado, A. (2005). SMEDWI-2 is a PIWI-like protein that regulates planarian stem cells. Science *310*, 1327–1330.

Rink, J.C., Gurley, K.A., Elliott, S.A., and Sánchez Alvarado, A. (2009). Planarian Hh signaling regulates regeneration polarity and links Hh pathway evolution to cilia. Science *326*, 1406–1410.

Roberts-Galbraith, R.H., and Newmark, P.A. (2013). Follistatin antagonizes activin signaling and acts with notum to direct planarian head regeneration. Proc. Natl. Acad. Sci. USA *110*, 1363–1368.

Rouhana, L., Weiss, J.A., Forsthoefel, D.J., Lee, H., King, R.S., Inoue, T., Shibata, N., Agata, K., and Newmark, P.A. (2013). RNA interference by feeding in vitro-synthesized double-stranded RNA to planarians: methodology and dynamics. Dev. Dyn. *242*, 718–730.

Saló, E., and Baguñà, J. (1984). Regeneration and pattern formation in planarians. I. The pattern of mitosis in anterior and posterior regeneration in *Dugesia (G) tigrina*, and a new proposal for blastema formation. J. Embryol. Exp. Morphol. *83*, 63–80.

Sánchez Alvarado, A., and Newmark, P.A. (1999). Double-stranded RNA specifically disrupts gene expression during planarian regeneration. Proc. Natl. Acad. Sci. USA *96*, 5049–5054.

Sánchez Alvarado, A., Newmark, P.A., Robb, S.M., and Juste, R. (2002). The *Schmidtea mediterranea* database as a molecular resource for studying platyhelminthes, stem cells and regeneration. Development *129*, 5659–5665.

Schindelin, J., Arganda-Carreras, I., Frise, E., Kaynig, V., Longair, M., Pietzsch, T., Preibisch, S., Rueden, C., Saalfeld, S., Schmid, B., et al. (2012). Fiji: an open-source platform for biological-image analysis. Nat. Methods *9*, 676–682.

Scimone, M.L., Lapan, S.W., and Reddien, P.W. (2014). A forkhead transcription factor is wound-induced at the planarian midline and required for anterior pole regeneration. PLoS Genet. *10*, e1003999.

Scimone, M.L., Cote, L.E., Rogers, T., and Reddien, P.W. (2016). Two FGFRL-Wnt circuits organize the planarian anteroposterior axis. eLife *5*, e12845.

Scimone, M.L., Cote, L.E., and Reddien, P.W. (2017). Orthogonal muscle fibres have different instructive roles in planarian regeneration. Nature *551*, 623–628.

Srivastava, M., Mazza-Curll, K.L., van Wolfswinkel, J.C., and Reddien, P.W. (2014). Whole-body acoel regeneration is controlled by Wnt and Bmp-Admp signaling. Curr. Biol. *24*, 1107–1113.

Stückemann, T., Cleland, J.P., Werner, S., Thi-Kim Vu, H., Bayersdorf, R., Liu, S.Y., Friedrich, B., Jülicher, F., and Rink, J.C. (2017). Antagonistic self-organizing patterning systems control maintenance and regeneration of the anteroposterior axis in planarians. Dev. Cell *40*, 248–263.e4.

Sureda-Gómez, M., Martín-Durán, J.M., and Adell, T. (2016). Localization of planarian β-CATENIN-1 reveals multiple roles during anterior-posterior regeneration and organogenesis. Development *143*, 4149–4160.

Tanaka, E.M., and Reddien, P.W. (2011). The cellular basis for animal regeneration. Dev. Cell *21*, 172–185.

van Wolfswinkel, J.C., Wagner, D.E., and Reddien, P.W. (2014). Single-cell analysis reveals functionally distinct classes within the planarian stem cell compartment. Cell Stem Cell *15*, 326–339.

Vásquez-Doorman, C., and Petersen, C.P. (2014). *zic-1* expression in planarian neoblasts after injury controls anterior pole regeneration. PLoS Genet. *10*, e1004452.

Vogg, M.C., Owlarn, S., Pérez Rico, Y.A., Xie, J., Suzuki, Y., Gentile, L., Wu, W., and Bartscherer, K. (2014). Stem cell-dependent formation of a functional anterior regeneration pole in planarians requires Zic and Forkhead transcription factors. Dev. Biol. *390*, 136–148.

Wenemoser, D., and Reddien, P.W. (2010). Planarian regeneration involves distinct stem cell responses to wounds and tissue absence. Dev. Biol. *344*, 979–991.

Wenemoser, D., Lapan, S.W., Wilkinson, A.W., Bell, G.W., and Reddien, P.W. (2012). A molecular wound response program associated with regeneration initiation in planarians. Genes Dev. *26*, 988–1002.

Witchley, J.N., Mayer, M., Wagner, D.E., Owen, J.H., and Reddien, P.W. (2013). Muscle cells provide instructions for planarian regeneration. Cell Rep. *4*, 633–641.

Wurtzel, O., Cote, L.E., Poirier, A., Satija, R., Regev, A., and Reddien, P.W. (2015). A generic and cell-type-specific wound response precedes regeneration in planarians. Dev. Cell *35*, 632–645.

Yazawa, S., Umesono, Y., Hayashi, T., Tarui, H., and Agata, K. (2009). Planarian Hedgehog/Patched establishes anterior-posterior polarity by regulating Wnt signaling. Proc. Natl. Acad. Sci. USA *106*, 22329–22334.

Zayas, R.M., Cebrià, F., Guo, T., Feng, J., and Newmark, P.A. (2010). The use of lectins as markers for differentiated secretory cells in planarians. Dev. Dyn. *239*, 2888–2897.

Zhang, X., Cheong, S.M., Amado, N.G., Reis, A.H., MacDonald, B.T., Zebisch, M., Jones, E.Y., Abreu, J.G., and He, X. (2015). Notum is required for neural and head induction via Wnt deacylation, oxidation, and inactivation. Dev. Cell *32*, 719–730.

Zhu, S.J., and Pearson, B.J. (2016). (Neo)blast from the past: new insights into planarian stem cell lineages. Curr. Opin. Genet. Dev. *40*, 74–80.

STAR★METHODS

KEY RESOURCES TABLE

REAGENT or RESOURCE	SOURCE	IDENTIFIER
Antibodies		
anti-digoxigenin-POD, Fab fragments	Roche	Cat# 11 207 733 910; RRID: AB_514500
anti-fluorescein-POD, Fab fragments	Roche	Cat# 11 426 346 910; RRID: AB_840257
anti-DNP-HRP conjugate	Perkin-Elmer	Cat# FP1129; RRID: AB_2629439
Anti-phospho-Histone H3 (Ser10) Antibody, clone 63-1C-8	Millipore	Cat# 05-817R; RRID:AB_11215621
Goat anti-rabbit antibody	ThermoFisher	Cat# 65-6120; RRID:AB_2533967
Chemicals		
TRIzol	Life Technologies	Cat#15596018
Western Blocking Reagent	Roche	Cat#11921673001
Critical Commercial Assays		
ApopTag Red *In Situ* Apoptosis Detection Kit	Millipore	Cat# S7165
Deposited Data		
follistatin RNAi RNaseq	Scimone et al., 2017	GEO: GSE99067
Smed_dd_v6 transcriptome	Brandl et al., 2016	http://planmine.mpi-cbg.de/planmine/begin.do
Experimental Models: Organisms/Strains		
Schmidtea mediterranea, clonal strain CIW4, asexual	Laboratory of Peter Reddien	N/A
Oligonucleotides		
Sequences used for all FISH probes and dsRNA provided in Table S1	N/A	N/A
Primers used for qRT-PCR are provided in Table S2	N/A	N/A
Software and Algorithms		
ImageJ (FIJI)	Schindelin et al., 2012	https://fiji.sc
ZEN digital imaging software	Zeiss	https://www.zeiss.com/microscopy/us/products/microscope-software/zen.html
GraphPad Prism	GraphPad Software	https://www.graphpad.com/scientific-software/prism/
R v.3.2.3	The R Foundation	https://www.r-project.org/
bowtie v1.1.2	Langmead et al., 2009	http://bowtie-bio.sourceforge.net/index.shtml
DESeq	Anders and Huber, 2010	https://bioconductor.org/packages/release/bioc/html/DESeq.html

CONTACT FOR REAGENT AND RESOURCE SHARING

Further information and requests for resources and reagents should be directed to and will be fulfilled by the Lead Contact, Dr. Peter Reddien (reddien@wi.mit.edu).

EXPERIMENTAL MODEL AND SUBJECT DETAILS

Asexual *Schmidtea mediterranea* strain animals (CIW4) were cultured in 1x Montjuic planarian water at 20° (Sánchez Alvarado et al., 2002). Animals were starved 1-2 weeks prior to experiments.

METHOD DETAILS

Double-stranded RNA synthesis for RNAi experiments

dsRNA was prepared from *in vitro* transcription reactions (Promega) using PCR-generated forward and reverse templates with flanking T7 promoters (TAATACGACTCACTATAGGG). Each template (16 μl) was mixed with 1.6 μl of 100 mM rNTPs (Promega); 0.6 μl of

1M dithiothreitol (DTT; Promega); 4 μl of T7 polymerase; and 24 μl of 5x Transcription optimized buffer (Promega). Reactions were incubated for 4h at 37°C. RNA was purified by ethanol precipitation, and re-suspended in a final volume of 30 μl milliQ H2O. Forward and reverse strands were combined and annealed by heating at 56°C followed by cooling to 37°C. Animals were starved for 1-2 weeks prior to first RNAi feeding and were fed twice a week. RNAi food mixture was prepared using 12 μl dsRNA for 30 μl planarian food (homogenized beef liver) (Rouhana et al., 2013). For RNAi of two or more genes, dsRNA for each gene was diluted in half (Scimone et al., 2016). For β-*catenin-1* double-RNAi experiments, animals were fed once with β-*catenin-1* or control dsRNA at the end of the feeding regimen. *C. elegans unc-22* was used as the control condition (Benian et al., 1989).

Double-stranded RNA injections for RNAi

dsRNA injections were performed using a Drummond Nanoject II Auto-nanoliter injector. Needles were pulled from Borosilicate capillaries (#BF100-78-15) on a Sutter Model P-2000 micropipette puller. Animals were injected 2-3 times with 32.9nl of dsRNA per injection.

Microsurgery

Head wedges were made by performing cuts from the medial point of the eye to the base of the auricle and the top of the head. Sagittal fragments were made with a single sagittal cut, immediately lateral to the pharynx. Pharynx resection was performed by creating a longitudinal dorsal incision followed by pharynx extraction. For serial cuts along the AP axis, AP cut 1 was made immediately posterior to the auricles, AP4 was made immediately anterior to the pharynx.

Fixation

Animals were killed in 5% NAC in PBS for 5 minutes before fixation in 4% formaldehyde for 15 minutes. Fixative was removed and worms were rinsed 2X with PBSTx (PBS + 0.1% Triton X-100). Animals were dehydrated and stored in methanol at −20°C. For Anti-phospho-Histone H3 labeling and TUNEL labeling, animals were not dehydrated after fixation (King and Newmark, 2013).

Whole-mount *in situ* hybridizations

RNA probes were synthesized as described previously (Pearson et al., 2009). Fluorescence *in situ* hybridizations (FISH) were performed as previously described (King and Newmark, 2013) with minor modifications. Briefly, fixed animals were bleached, rehydrated and treated with proteinase K (2 μg/ml) in 1xPBSTx. Following overnight hybridizations, samples were washed twice in pre-hyb solution, 1:1 pre-hyb-2X SSC, 2X SSC, 0.2X SSC, PBSTx. Subsequently, blocking was performed in 0.5% Roche Western Blocking reagent and 5% inactivated horse serum in 1xPBSTx. Animals were incubated in antibody overnight at 4°C. Post-antibody washes and tyramide development were performed as described (King and Newmark, 2013). Peroxidase inactivation was done in 1% sodium azide for 90 minutes at RT. Specimens were counterstained with DAPI overnight (*Sigma*, 1 μg/ml in PBSTx).

phospho-Histone H3 labeling

Fixed animals were bleached overnight at room temperature in H_2O_2 (*Sigma,* 6% in 1xPBSTx). Bleached animals were permeabilized in Proteinase K solution (2 μg/ml in 1xPBSTx with 0.1% SDS) and post-fixed in formaldehyde (4% in 1xPBSTx). Animals were placed in anti-phospho-Histone H3 antibody (*Millipore 05-817R-I, clone 63-1C-8*) overnight at room temperature at a concentration of 1:300 in 5% inactivated horse serum. Samples were washed with PBSTx, then placed in goat anti-rabbit antibody (*ThermoFisher 65-6120*) overnight at room temperature at 1:300 in 5% inactivated horse serum. After PBSTx washes, samples were developed in fluorescein tyramide (1:3000 in PBSTx, with 0.003% H_2O_2) for 10 minutes at room temperature. Samples were washed in PBSTx and labeled with DAPI (*Sigma*, 1 μg/ml in PBSTx) before mounting.

TUNEL

TUNEL was performed using reagents from the ApopTag Red *In Situ* Apoptosis Detection Kit (*Millipore*, #S7165). Fixed animals were bleached overnight at room temperature in H_2O_2 (*Sigma,* 6% in PBSTx). Bleached animals were permeabilized in Proteinase K solution (2 μg/ml in PBSTx with 0.1% SDS) and post-fixed in formaldehyde (4% in PBSTx). Samples were transferred to 1.5mL micro centrifuge tubes. PBSTx was replaced with 20 μL reaction mix (3 parts ApopTag TdT enzyme mix, 7 parts ApopTag reaction buffer), and incubated overnight at 37°C. Animals were washed in PBSTx followed by development in 20 μL development solution (1 part blocking solution, 1 part ApopTag anti-digoxigenin rhodamine conjugate), and incubated in the dark at room temperature overnight. Samples were washed in PBSTx and counterstained with DAPI (*Sigma*, 1 μg/ml in PBSTx). TUNEL protocol was adapted from previous work (Pellettieri et al., 2010).

Quantitative real-time PCR (qRT-PCR)

Three to five animals were collected per biological replicate with three biological replicates per condition. Total RNA was isolated in 1mL Trizol (*Life Technologies*) as per manufacturer's instructions. Samples were triturated using a P1000 tip to homogenize tissue. Following RNA purification and resuspension in MilliQ H_2O, concentrations for each sample were determined using the Qubit RNA HS Assay Kit (*Life Technologies*). 1μg RNA input was used to prepare cDNA with the SuperScript III Reverse Transcriptase kit (*Invitrogen*). Ct values from three technical replicates were averaged and normalized by the Ct value of the housekeeping gene *g6pd* to

generate ΔCt values. Relative expression levels were determined by the -ΔΔCt method by calculating the difference from the average ΔCt value of control RNAi replicates. Bar graphs show relative expression values as $2^{-\Delta\Delta CT}$ with standard deviation and individual expression values. Primer pairs used are provided in Table S2.

RNA sequencing Analysis

RNaseq data for *follistatin* RNAi tail regeneration was analyzed from previously published experiments (Scimone et al., 2017) (GEO: GSE99067). Reads were mapped to the dd_Smed_v6 transcriptome (Brandl et al., 2016) (http://planmine.mpi-cbg.de/planmine/begin.do) using bowtie-1 (Langmead et al., 2009). Raw read counts were subjected to independent filtering with the filter criterion, overall sum of counts, to remove genes in the lowest 40% quantile. Differential expression analysis was performed using DEseq (Anders and Huber, 2010). Heatmaps were generated using pheatmap and are displayed as $\log_2$Fold change values. Genes without a best BLAST hit are identified by transcriptome ID (dd_xxx) in heatmaps. Significance is reported as p_{adj} values, with $p_{adj} < 0.05$ used as a cutoff.

Microscopy and image analysis

Fluorescent images were taken with a Zeiss LSM700 Confocal Microscope. All images are Maximum intensity projections. Images of samples that did not fit the microscope field of view were obtained using the tile scan function (Zeiss ZEN) that aligns and stitches tiles to obtain a single image of a large specimen. Images were processed using ImageJ (Fiji) (Schindelin et al., 2012). Light images were taken with a Zeiss Discovery Microscope. Cell counting was performed manually after blinding control and experimental conditions.

QUANTIFICATION AND STATISTICAL ANALYSIS

Statistical analyses were performed using the Prism software package (GraphPad Inc., La Jolla, CA). Comparisons between the means of two populations were done by a Student's t test. Comparisons of means between multiple populations were done by one-way ANOVA. Comparisons between means of time-points in a time course was done by two-way ANOVA. Significance was defined as $p < 0.05$. Statistical tests, significance, data points, error bars and animal numbers (n) for each figure are provided in the legends.